

## Intercalation in Layered Metal–Organic Frameworks: Reversible Inclusion of an Extended $\pi$ -System

Hasan K. Arslan,<sup>†</sup> Osama Shekhah,<sup>†</sup> D.C. Florian Wieland,<sup>‡</sup> Michael Paulus,<sup>‡</sup> Christian Sternemann,<sup>‡</sup> Martin A. Schroer,<sup>‡</sup> Sebastian Tiemeyer,<sup>‡</sup> Metin Tolan,<sup>‡</sup> Roland A. Fischer,<sup>||</sup> and Christof Wöll<sup>†,\*</sup>

<sup>†</sup>Karlsruhe Institute of Technology, Institute of Functional Interfaces (IFG), Hermann-von-Helmholtz-Platz 1, 76344 Eggenstein-Leopoldshafen, Germany

<sup>‡</sup>Technische Universität Dortmund, Fakultät Physik/DELTA, 44221 Dortmund, Germany

<sup>||</sup>Inorganic Chemistry II, Ruhr University Bochum, Bochum, Germany

 Supporting Information

**ABSTRACT:** We report the synthesis of layered  $[\text{Zn}_2(\text{bdc})_2(\text{H}_2\text{O})_2]$  and  $[\text{Cu}_2(\text{bdc})_2(\text{H}_2\text{O})_2]$  (bdc = benzdicarboxylate) metal–organic frameworks (MOF) carried out using the liquid-phase epitaxy approach employing self-assembled monolayer (SAM) modified Au-substrates. We obtain Cu and Zn MOF-2 structures, which have not yet been obtained using conventional, solvothermal synthesis methods. The 2D  $\text{Cu}^{2+}$  dimer paddle wheel planes characteristic for the MOF are found to be strictly planar, with the planes oriented perpendicular to the substrate. Intercalation of an organic dye, DXP, leads to a reversible tilting of the planes, demonstrating the huge potential of these surface-anchored MOFs for the intercalation of large, planar molecules.

The present large interest in metal–organic frameworks (MOFs) results from the fact that these highly porous and highly ordered materials can be used for a variety of different applications ranging from gas storage over catalysis and sensing to drug release.<sup>1–4</sup> A fascinating aspect of this huge class of crystalline porous materials constructed from metal-oxo nodes and organic struts, with now more than 1000 different realizations known, is the fact that a number of guide principles allow us to describe the vast amount of different structures with a fairly small number of structural motifs, e.g. in the case of reticular MOFs.<sup>5,6</sup> These guide principles make it possible to design new frameworks with tailored functionalities. If, for example, the MOF should bind a particular molecule in the pores of the framework, one can choose a structural motif and then modify the ligands previously used to fabricate other instances of this particular MOF by attaching specific functionalities. If changes do not affect the binding of the ligand to the metal-oxo node, the MOF will grow and exhibit the desired functionality, either immediately or by employing a postsynthesis modification.<sup>7</sup>

One of the most important structural motifs in the architecture of MOFs is the 4-fold coordinated dimetal-centered paddle wheel, important realizations being based either on Cu ( $[\text{Cu}_3(\text{btc})_2]$ ,  $[\text{Cu}_2(\text{bdc})_2(\text{dabco})]$ ,  $[\text{Cu}_2(\text{bdc})_2(\text{bipy})]$ ) or on Zn ( $[\text{Zn}_2(\text{bdc})_2(\text{dabco})]$ ,  $[\text{Zn}_2(\text{bdc})_2(\text{bipy})]$ ).<sup>1,8</sup> In fact, within the reticular class of MOFs the Zn-bdc (MOF-2) system was one of the first reported.<sup>9</sup> The structure of MOFs constructed using

this node–ligand binding is based on the 4-fold connectivity of the metal dimers<sup>10</sup> (Figure 1). Depending on the number of connectivities of the ligand, e.g. two in the case of 1,4-benzenedicarboxylic acid ( $\text{H}_2\text{bdc}$ ) and three in the case of 1,3,5-benzenetricarboxylic acid ( $\text{H}_3\text{btc}$ ), layered two- or three-dimensional frameworks can be obtained.

The simplest realization of an MOF based on such a 4-fold paddle-wheel structure would be an array of planar, strictly quadratic paddle wheels forming layers with a 4-fold symmetry (Figure 1, center), with the layers stacked regularly on top of each other via a bonding of the  $\text{M}^{2+}$  ions through e.g. water-mediated hydrogen bonds (Figure 1, right), yielding the high-symmetry tetragonal space group  $P4/nbm$ . Such a layered MOF would be of interest with regard to intercalation, e.g. the embedding of large, planar  $\pi$ -systems. The size of an important dye,  $N,N'$ -bis(2,6-dimethylphenyl)-3,4:9,10-perylenetetracarboxylic di-imide (DXP),<sup>11</sup> amounts to 2.1 nm, which exceeds the pore sizes typically available within most MOFs.

Interestingly, however, despite significant effort a successful synthesis of this fundamental and important MOF-2 basic structure has not been reported yet. In the case of Zn, the reported structure of  $[\text{Zn}(\text{bdc})(\text{H}_2\text{O})(\text{dmf})]$  (dmf =  $N,N$ -dimethylformamide) which is known as MOF-2,<sup>9,12</sup> contains layers with 4-fold symmetry, but these layers are stacked in a shifted (staggered) fashion, yielding a monoclinic 3D crystal structure with a  $P1_2/n$  space group. The shift in the stacking results from the interlayer interactions brought about by a water molecule inducing an asymmetric interaction, the water hydrogen forming a hydrogen bond with a  $\text{Zn}^{2+}$  ion and the other with an oxygen atom of a carboxylate group. In the case of Cu the success is even less encouraging. Although an MOF-2 analogue with Cu was proposed by Mori et al.,<sup>13</sup> no XRD data allowing for a structure determination were reported in this early work. Recently, Tannenbaum et al.<sup>14</sup> reported the synthesis of  $[\text{Cu}(\text{bdc})(\text{dmf})]$  (MOF-2 analogue) with a  $C2/m$  space group. A structural analysis could only be carried out for the dmf-loaded framework. For the empty framework the structure could not be determined since the desolvation process only left a fine powder with XRD peaks of low quality. It thus appears that interlayer interactions brought about by the solvent molecules ( $\text{H}_2\text{O}$  in case of MOF-2, dmf in the

Received: April 25, 2011

Published: May 02, 2011

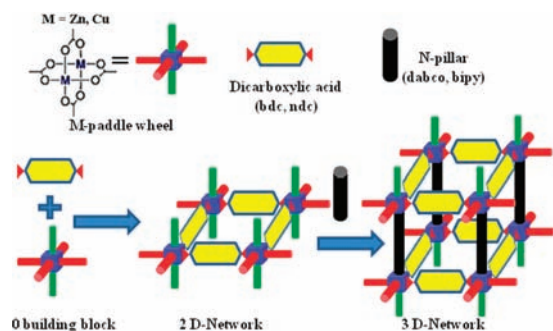


**Figure 1.** Schematic representation of the synthesis and formation of the 2 and 3D paddle wheel layered based metal–organic frameworks (LBMOFs).

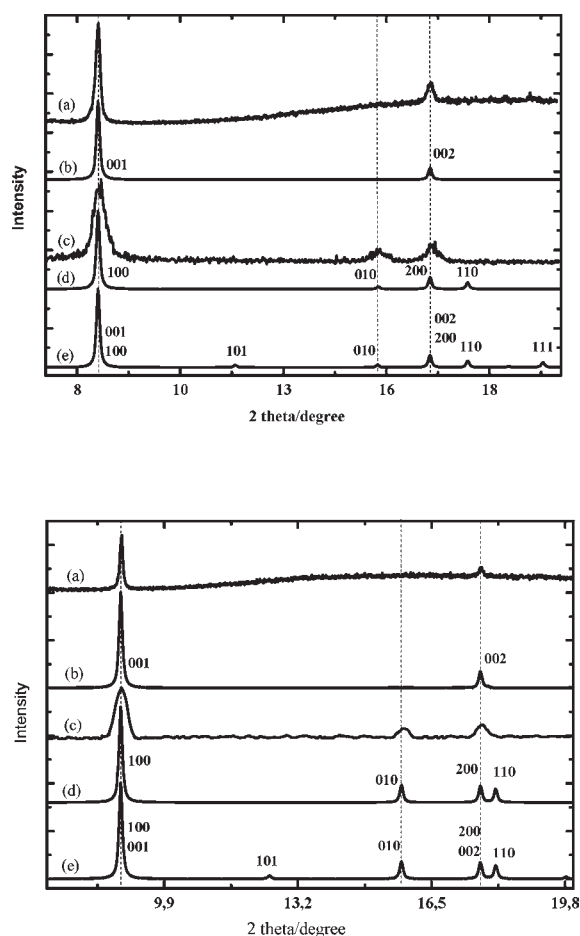


**Figure 2.** X-ray diffraction patterns of  $[\text{Zn}_2(\text{bdc})_2(\text{H}_2\text{O})_2]$  (upper) and  $[\text{Cu}_2(\text{bdc})_2(\text{H}_2\text{O})_2]$  (down) SURMOFs: (a) Out-of-plane (experimental), (b) Out-of-plane (calculated), (c) In-plane (experimental), (d) In-plane (calculated), and (e) Bulk (calculated).

case of the Cu-analogue to MOF-2) prohibit the formation of the ideal (Cu,Zn)-bdc MOF with  $P4/nbm$  symmetry. This speculation is supported by the fact that by introducing appropriate pillar molecules, e.g. dabco or bipyridin, a regular stacking of the paddle-wheel layers can be achieved.<sup>1</sup>

In the present study we have employed a novel method to synthesize metal–organic frameworks, which is based on liquid

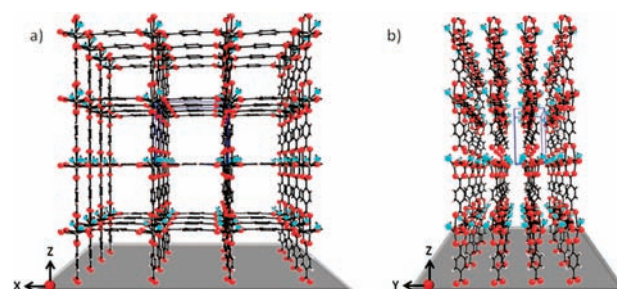


**Figure 3.** Schematic representation of the proposed 2D structure of SURMOFs  $[\text{Zn}_2(\text{bdc})_2(\text{H}_2\text{O})_2]$  and  $[\text{Cu}_2(\text{bdc})_2(\text{H}_2\text{O})_2]$ ; (a) front view and (b) side view. In both cases a  $P4$  space group with a simple tetragonal unit cell is assumed.

phase epitaxy (LPE) on a templating substrate.<sup>15,16</sup> Briefly, the LPE process is a layer-by-layer procedure, where appropriately functionalized substrates are immersed into solutions of the reactants in a sequential fashion (Figure S1). Whereas in many cases the structure of the MOF thin films yielded from the LPE method is identical to that of the bulk ( $[\text{Cu}_3(\text{btc})_2]$ ,  $[\text{Cu}_2(\text{ndc})_2(\text{dabco})]$ ,...) in other cases it has been shown that with LPE pseudomorphs of MOFs can be obtained, which are not accessible via conventional synthesis methods, e.g. a noninterpenetrated version of MOF 508b.<sup>15,17</sup>

The X-ray diffraction (XRD) patterns shown in Figure 2a and b directly demonstrate that the LPE method yields films with an MOF-2 structure with  $P4$  symmetry for Zn and an MOF-2 analogue with the same comparably high symmetry in the case of Cu. The XRD data recorded in the direction perpendicular to the surface (out-of-plane scans) show only the (001) diffraction peak. The position of this peak allows us to determine the size of the paddle-wheel squares; the value of 10.01 Å for Zn is in excellent agreement with that reported in previous studies.<sup>1</sup> The fact that no other diffraction peaks are seen in this direction reveals that the paddle-wheel planes grow perpendicular to the templating organic substrate, (Figure 3). The in-plane XRD-scans recorded at grazing incidence (scattering vector parallel to surface) reveal only one additional diffraction peak, a (010) peak. The fact that the (100) and (001) diffraction peaks are located at identical positions directly demonstrates that the planes are regularly stacked yielding a simple tetragonal unit cell. Any distortion of the unit cell would yield different positions of the (001) peak in the out-of-plane and of the (100) peak in the in-plane diffraction data. Note also that any staggered stacking of the planes would result in a monoclinic unit cell, which is not compatible with the  $P4$  symmetry.

In fact, an ideal MOF-2 structure with  $P4$  symmetry and a simple tetragonal unit cell for both, Cu and Zn, with the 2D paddle-wheel layers stacked regularly and orientated normal to the substrate (Figure 3) is fully consistent with these data. For Zn, a value of 10.01 Å is found for the  $a$  and  $b$  parameters of the simple tetragonal unit cell, which is smaller than 12.43 Å reported for the monoclinic unit cell in Zn-based MOF-2 by Li et al.<sup>9</sup> From the position of the (010) diffraction peak we conclude that the distance between the layers amounts to 5.6 Å, a value which is larger than the interplanar spacing observed for MOF-2 reported by Li et al. ( $\sim 2$  Å) but smaller than other Zn paddle wheel based LBMOFs like  $[\text{Zn}_2(\text{bdc})_2(\text{dabco})]$ , for which the spacing amounts to 9.6 Å.<sup>9</sup>

The Cu-MOF-2 polymorph reported by Tannenbaum and co-workers<sup>14</sup> contains an oblique unit cell, with  $a = 14.269$  Å and

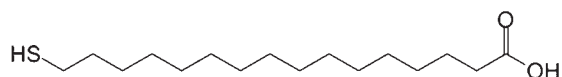


**Figure 4.** Chemical structure of 16-mercaptohexadecanoic acid (MHDA) SAM.

$c = 11.414 \text{ \AA}$ . For the Cu MOF-2 produced using LPE, we propose a structure analogous to Zn, with  $a = c = 10.61 \text{ \AA}$  and  $b = 5.8 \text{ \AA}$ . In the case of the LBMOF  $[\text{Cu}_2(\text{bdc})_2\text{dabco}]$ , the spacing between the Cu paddle-wheel sheets amounts to  $9.6 \text{ \AA}$ . This value is given by the length of the dabco pillars connecting the Cu dimers in the  $[001]$  crystallographic direction and is, not surprisingly, much larger than the value reported here. In the present case the sheets are not connected together directly using single molecule pillars but by water molecules hydrogen-bonded to the axial positions of the paddle wheel. The water molecules were clearly seen in IR data (Figure S2 in the Supporting Informations).

Also in (Figure 2) we present the results of a simulation of the lattice diffraction peaks assuming an ideal structure for (Cu,Zn) MOF-2 analogues as shown in (Figure 3). The agreement between the experimental and theoretical relative diffraction peak intensities is very good.

In order to investigate the effect of solvent removal we have studied the variation of the diffraction patterns as a function of temperature upon heating in vacuum. The data (Figures S3 and S4) reveal no changes of peak positions for temperatures of up to  $240 \text{ }^\circ\text{C}$ ; above  $120 \text{ }^\circ\text{C}$  a slight attenuation of diffraction peak intensities is seen. Between  $240$  and  $290 \text{ }^\circ\text{C}$  the solvent molecules are released, which is accompanied by a small shift ( $0.2^\circ$ ) of the  $[001]$  reflection to higher Bragg angles. After cooling the sample in vacuum back to room temperature the shift is conserved. Subsequent exposure to air results in an XRD pattern identical to the initial one. These experiments reveal that the SURMOFs are stable with regard to the removal of solvent molecules without losing crystallinity and long-range order.

The perpendicular orientation of the 2D metal-bdc planes with respect to the surface can be explained by the paddle wheel units being anchored to the surface by replacing one of the four bdc-carboxylate units occurring within the bulk structure by a surface carboxylate group exposed by the COOH-terminated 16-mercaptohexadecanoic acid (MHDA) SAM (Figure 4).

This anchoring naturally leads to a structure where the planar sheets are oriented perpendicular to the substrate surface (Figure 3). A similar anchoring has been proposed for HKUST-I SURMOFs grown on COOH-terminated SAMs.<sup>15,18</sup> The exceptional high quality of the out-of-plane diffraction scans and in particular the absence of the  $(010)$  peak (which is clearly visible in the in-plane diffraction data) reveal that this perpendicular orientation is strongly preferred. In addition, related SURMOFs of the type  $[\text{M}_2\text{L}_2\text{P}]$  ( $m = \text{Zn, Cu}$ ;  $\text{L} = \text{bdc, ndc}$ ;  $\text{P} = \text{dabco, bipy}$ ) can be grown by LPE in the same  $[100]$  orientation on COOH terminated SAMs by choosing appropriate conditions.<sup>19</sup>

An intriguing option of the perpendicular planes is to use them for intercalation of larger, planar aromatic molecules. We demonstrate the huge potential of the surface-anchored MOF-2 described here with regard to such an intercalation by a loading experiment with an important organic dye, DXP. After removing the solvent as described above the Cu MOF-2 was immersed in an ethanolic solution of DXP at  $50 \text{ }^\circ\text{C}$ . After 48 h the color changes indicated inclusion of the dye (Figure S5), and the corresponding

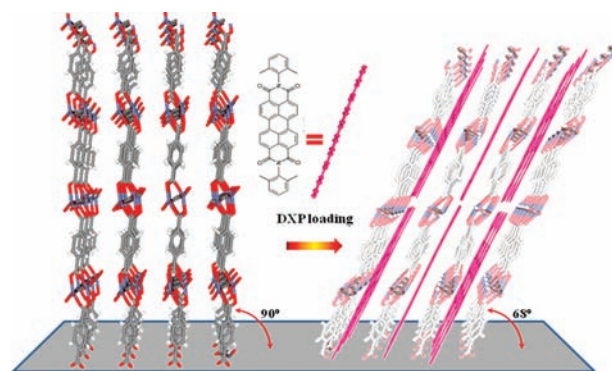


**Figure 5.** Side view schematic representation of the 2D structure of SURMOFs  $[\text{Cu}_2(\text{bdc})_2(\text{H}_2\text{O})_2]$  before and after loading with DXP (water molecules were omitted for reasons of clarity).

XRD patterns (Figure S6) revealed the presence of new diffraction peaks labeled  $001(\text{I})$  and  $002(\text{I})$ , demonstrating the presence of a new crystalline structure. We propose that the new structure is formed by a slight tilting ( $32^\circ$ ) of the paddle-wheel planes away from the surface normal to increase the interaction with the intercalated planar DXP (Figure 5). This tilting shifts the  $(001)$  diffraction peak from the position of the  $(100)$  peak to a slightly higher value. Further experiments showed that the loading with DXP is fully reversible (Figure S5).

We speculate that the reason for obtaining ideal MOF-2 structures for both Cu and Zn, with the LPE process—but not with the conventional solvothermal process—results from anchoring of the carboxylate units to the templating surface, which renders lateral shifts of the paddle-wheel planes energetically very unfavorable. A similar effect of the organic templating surface stabilizing an MOF pseudomorph not accessible via bulk synthesis methods has been reported recently for the case of  $[\text{Zn}_2(\text{bdc})_2(\text{bipy})]$  (MOF-508), where an LPE growth on a pyridine-terminated organic surface yielded a noninterpenetrated pseudomorph of this layer-pillar MOF.<sup>17</sup>

In conclusion we have demonstrated that the idealized MOF-2 structure, for which a synthesis using the conventional route is either difficult (reaction times of several weeks) or impossible, can be readily prepared for both Cu and Zn, by using a liquid phase epitaxy scheme involving a layer-by-layer deposition on a templating organic surface. The layered MOF-2 is very well suited for intercalation of large, aromatic molecules as demonstrated for the case of DXP.

This result implies that at least for LBMOFs the LPE method is very well suited to grow model and references systems, but certainly also for applications where a high degree of ordering and crack-free coating of solid substrates are needed (Figure S7). The  $[100]$  oriented layered SURMOFs of the general formula  $[\text{M}_2\text{L}_2(\text{H}_2\text{O})_2]$  as analogues of MOF-2 exhibit a number of interesting properties over e.g. layer-pillar SURMOFs such as  $[\text{M}_2\text{L}_2\text{P}]$ .<sup>19</sup> For example, the water molecule at the axial position of the metal dimers may be replaced after completion of the LPE process, i.e. SURMOF activation, which means that the metal sites can be made available for binding of guest molecules and for catalytic applications.

## ■ ASSOCIATED CONTENT

**S Supporting Information.** Experimental procedures, IR-RAS, XRD, light microscopy images, and AFM images are included

in the Supporting Information. This material is available free of charge via the Internet at <http://pubs.acs.org>.

## AUTHOR INFORMATION

### Corresponding Author

christof.woell@kit.edu

## ACKNOWLEDGMENT

We acknowledge the DELTA machine group for providing synchrotron radiation. This work was supported by the German Research Foundation within the Priority Program 1362 on Metal Organic Frameworks. We also acknowledge financial support from the NRW Forschungsschule "Forschung mit Synchrotronstrahlung in den Nano- und Biowissenschaften".

## REFERENCES

- (1) Kitagawa, S.; Kitaura, R.; Noro, S. *Angew. Chem., Int. Ed.* **2004**, *43*, 2334–2375.
- (2) Ferey, G. *Chem. Soc. Rev.* **2008**, *37*, 191–214.
- (3) Rowsell, J.; Yaghi, O. *Microporous Mesoporous Mater.* **2004**, *73*, 3–14.
- (4) Kuppler, R. J.; Timmons, D. J.; Fang, Q. R.; Li, J. R.; Makal, T. A.; Young, M. D.; Yuan, D. Q.; Zhao, D.; Zhuang, W. J.; Zhou, H. C. *Coord. Chem. Rev.* **2009**, *253*, 3042–3066.
- (5) Eddaoudi, M.; Li, H. L.; Yaghi, O. M. *J. Am. Chem. Soc.* **2000**, *122*, 1391–1397.
- (6) O'Keeffe, M.; Eddaoudi, M.; Li, H. L.; Reineke, T.; Yaghi, O. M. *J. Solid State Chem.* **2000**, *152*, 3–20.
- (7) Savonnet, M.; Bazer-Bachi, D.; Bats, N.; Perez-Pellitero, J.; Jeanneau, E.; Lecoq, V.; Pinel, C.; Farrusseng, D. *J. Am. Chem. Soc.* **2009**, *132*, 4518–4519.
- (8) Mori, W.; Takamizawa, S.; Kato, C. N.; Ohmura, T.; Sato, T. *Microporous Mesoporous Mater.* **2004**, *73*, 31–46.
- (9) Li, H.; Eddaoudi, M.; Groy, T. L.; Yaghi, O. M. *J. Am. Chem. Soc.* **1998**, *120*, 8571–8572.
- (10) Braun, M. E.; Steffek, C. D.; Kim, J.; Rasmussen, P. G.; Yaghi, O. M. *Chem. Commun.* **2001**, 2532–2533.
- (11) Muller, M.; Devaux, A.; Yang, C. H.; De Cola, L.; Fischer, R. A. *Photochem. Photobiol. Sci.* **2010**, *9*, 846–853.
- (12) Mueller, U.; Schubert, M.; Teich, F.; Puetter, H.; Schierle-Arndt, K.; Pastre, J. J. *Mater. Chem.* **2006**, *16*, 626–636.
- (13) Seki, K.; Takamizawa, S.; Mori, W. *Chem. Lett.* **2001**, *30*, 122–123.
- (14) Carson, C. G.; Hardcastle, K.; Schwartz, J.; Liu, X. T.; Hoffmann, C.; Gerhardt, R. A.; Tannenbaum, R. *Eur. J. Inorg. Chem.* **2009**, *2009*, 2338–2343.
- (15) Shekhah, O.; Wang, H.; Kowarik, S.; Schreiber, F.; Paulus, M.; Tolan, M.; Sternemann, C.; Evers, F.; Zacher, D.; Fischer, R. A.; Wöll, C. *J. Am. Chem. Soc.* **2007**, *129*, 15118–15119.
- (16) Shekhah, O. *Materials* **2010**, *3*, 1302–1315.
- (17) Shekhah, O.; Wang, H.; Paradinas, M.; Ocal, C.; Schupbach, B.; Terfort, A.; Zacher, D.; Fischer, R. A.; Wöll, C. *Nat. Mater.* **2009**, *8*, 481–484.
- (18) Shekhah, O.; Wang, H.; Zacher, D.; Fischer, R. A.; Wöll, C. *Angew. Chem., Int. Ed.* **2009**, *48*, 5038–5041.
- (19) Zacher, D.; Yussenko, K.; Betard, A.; Meilikhov, M.; Ladnorg, T.; Shekhah, O.; Terfort, A.; Wöll, C.; Fischer, R. A. *Chem.—Eur. J.* **2011**, *17*, 1448–1455.